Pseudolocal modes of guest molecules in mixed molecular crystals: Photon echo experiments and computer simulations

R. W. Olson
IBM Palo Alto Scientific Center, Palo Alto, California 94304

Jeffrey S. Meth, C. D. Marshall, Vincent J. Newell, and M. D. Fayer
Department of Chemistry, Stanford University, Stanford, California 94305

(Received 26 October 1989; accepted 15 December 1989)

The temperature-dependent optical dephasing of anthracene, 9-methylanthracene, and 2-methylanthracene monomers in phenanthrene host crystals has been measured using photon echo experiments. Despite large linear electron–acoustic phonon coupling, all three systems dephase because of coupling to pseudolocal modes (local motions of the guest molecule). Computer simulations of the three systems calculate the pseudolocal mode eigenvalues and eigenvectors. In contrast to previous discussions in the literature which describe pseudolocal modes as librations, the predicted eigenvalues are in reasonable agreement with the measured pseudolocal mode energies. The predicted eigenvectors are combinations of translational motion along the long molecular axis and rotational motion about the out-of-plane axis of the guest. Differences in site energies for various locations and orientations of the methyl group are calculated.

I. INTRODUCTION

Understanding the interactions between electronic states and bath states in a medium is important for several reasons. The phenomenon occurs throughout nature. The mechanism of photosynthesis, the characteristics of lasing materials, and the functioning of proteins and membranes in biological systems[1–3] all depend on details of the interactions between electronic and mechanical degrees of freedom. Changes in electronic states cause changes in the nuclear motions, and the nuclear motions in turn perturb the electronic states. Understanding these interactions will help unravel the fundamental nature of the modes of molecules embedded in solids of all types: crystals, glasses, proteins, and polymers. In this paper we examine the detailed properties of the motion of molecules contained in a crystalline host with photon echo experiments and computer simulations. While the experiments are performed on crystals, the results have implications for all condensed matter systems.

The mechanisms of electronic dephasing of monomeric impurities in crystals have been described theoretically. McCumber and Sturge discussed the dephasing of the Cr^{+3} ion in Al_2O_3 (ruby).[4] In the 1970's, the work was advanced by Osad'ko,[5] Harris,[6] Small,[7] and de Bree and Wiersma.[8] The most complete theory was developed by Skinner and Hsu in the mid 1980's.[9] It is known that quadratic coupling between the electronic states and the mechanical degrees of freedom is responsible for dephasing. The Skinner–Hsu theory uses a many-body cumulant expansion to express the dephasing as an integral involving the density of phonon states and coupling constants. The infinite order theoretical expressions can be evaluated numerically to yield the rate of dephasing as a function of temperature. Certain approximations, however, are useful. The phonons are divided into three types: optical, acoustic, and pseudolocal. Optical and acoustic phonons involve motions of the bulk crystal degrees of freedom, and exist in the absence of guest molecules. A pseudolocal phonon is a motion which is largely localized on a guest molecule in the host lattice. In the absence of any coupling to the lattice degrees of freedom, the guest would have strictly localized modes. Weak coupling with bulk phonons slightly mixes the localized guest modes with bulk phonons, yielding pseudolocal modes.

It is possible to calculate analytically the optical dephasing (optical line broadening) of the guest electronic states arising from coupling to each of these three types of phonons. Dephasing caused by coupling to a Debye model of acoustic phonons has a T^7 temperature dependence.[9,10] Coupling to a pseudolocal mode results in an exponentially activated temperature dependence.[9] Coupling to optical phonons produces an approximately exponentially activated temperature dependence.[9] In the pseudolocal case, the activation energy corresponds to the pseudolocal phonon energy, while in the optical phonon case, the apparent activation energy depends on the phonon frequency, the band width and the functional form of the density of states.

Experimentally, the dephasing is manifested in the homogeneous linewidth (frequency domain) or the transverse relaxation time, T_2 (time domain). The simplest frequency domain experiment is linear absorption spectroscopy. Measuring the linewidth as a function of temperature, while simple in principle, is often impossible in practice because of inhomogeneous broadening. Inhomogeneous broadening arises from strains, disorder, and defects in the sample. Each guest experiences a slightly different energy shift in going from the gas phase into the solid state because of varying host environments. At low temperatures, this inhomogeneous width, on the order of wave numbers, obscures the homogeneous width, on the order of megahertz to gigahertz, making linear spectroscopy impractical in most systems. McCumber and Sturge were able to measure T_2 in ruby using

 0021-9606/90/063323-12$03.00

absorption spectroscopy above ~77 K. Below that temperature, inhomogeneous broadening masked the homogeneous linewidth. In general, inorganic crystals are more amenable to linear spectroscopy in this fashion than are organic crystals.[11]

In the time domain, the photon echo technique[12,13] can be used to measure T_2. The two pulse photon echo removes inhomogeneous broadening from the linewidth (polarization decay) and provides the Fourier transform of the homogeneous absorption line. Lorentzian homogeneous lines give rise to exponential echo decays and are observed in the experiments presented below. The echo decay measurements yield T_2, the optical dephasing time (transverse relaxation time), and $1/\pi T_2$ in the homogeneous linewidth. In the absence of fluctuations of the medium, the dephasing time is determined by the excited state lifetime, T_1. Phonon induced dephasing decreases T_2 below its maximum $T_2 = 2T_1$.

McCumber and Sturge have shown that the dephasing in ruby is caused by coupling of the Cr^{+3} ion to acoustic phonons.[4] Photon echo work done by Hesselink and Wiersma[14] and by Patterson *et al.*[15] on monomeric and dimeric impurities in molecular crystals has demonstrated that pseudolocal modes are responsible for dephasing in these systems.

The pseudolocal modes correspond to the six external degrees of freedom a molecule has in the gas phase, three translational and three rotational. In the crystal three become translational and three become librational (hindered rocking) modes. These are analogous to acoustic phonons and librons (optical phonons) in pure crystals. In an atomic system such as ruby, the Cr^{+3} cannot possess librational degrees of freedom. In the molecular systems studied, these modes do exist and it was postulated that the pseudolocal mode was librational in character.[14,15] Proving this hypothesis is not easy. Hesselink and Wiersma,[14] who studied pentacene and perdeuterated pentacene in naphthalene, compared the energies of absorption peaks in the phonon side band with the calculated moments of inertia for the two guests. They concluded that the dephasing was librational, but were not able to determine about which axis the guest librated. However, the change in mass upon deuteration would cause a similar change in translational mode frequencies. They argued against a translational degree of freedom being responsible for the dephasing by suggesting that translational motions would be amalgamated into the acoustic phonon bands. The temperature-dependent photon echo experiment measures the pseudolocal phonon energy, but it cannot associate that energy with a particular motion in the system.

Computer simulations have been performed on numerous molecular systems to study the local structure[16] and to characterize the possible pseudolocal modes.[17] In this paper we present simulations which are unique because they allow translational and librational degrees of freedom for the guest and permit mixed motions as well. Earlier studies allowed only librational degrees of freedom.[17]

A systematic study of the optical dephasing of three chromophores in the same host and computer simulations of the same three systems provides detailed insights into the nature of pseudolocal modes. The host used was phenanthrene, and the guests were: anthracene, 9-methylanthracene, and 2-methylanthracene. The anthracene system was chosen for several reasons. First, it is a structural isomer of phenanthrene, and goes into the lattice very well. By placing substituent groups on the anthracene, it should be possible to determine the motion of the pseudolocal mode by correlating the changes in mass, moments of inertia of the chromophore, and local structure of the host with changes in the experimentally determined activation energies. Second, unlike previously studied systems, these systems have a large phonon sideband, with a Debye–Waller factor of about unity. This demonstrates strong linear excitation-phonon coupling. If systems with strong linear coupling also tended to exhibit strong quadratic coupling, quadratic coupling to acoustic phonons could compete with quadratic coupling to pseudolocal modes.

Picosecond photon echoes on these systems in the temperature range 1–15 K confirm that pseudolocal mode dephasing is dominant at low temperatures and yield the pseudolocal mode energies. Comparison of the experimental results to the computer simulations reveals the nature of the pseudolocal modes responsible for optical dephasing. We find that the pseudolocal mode is a mixture of librational and translational motion, and in two of the systems studied, the translational motion is dominant. The translation occurs along the long axis of the molecule, while the libration occurs about the out-of-plane axis of the molecule. The computer simulations also provide information on the structures of distinct guest configurations in the host lattice.

II. EXPERIMENTAL METHODS

The experimental setup for performing the photon echoes is shown in Fig. 1. A Q-switched, mode-locked, Nd:YAG laser run at 0.5 KHz produces a pulse train of 80 ps, 1.064 μm pulses. A single IR pulse is selected from the pulse train with a Pockels cell and the remainder of the pulse train is doubled to 532 nm and used to synchronously pump a dye laser. The dye laser is cavity dumped and the dye pulse is summed with the IR single pulse to produce a 30 ps pulse of roughly 5 μJ, tunable from 365–415 nm. This near-UV pulse is split into the π and $\pi/2$ pulses. The π pulse is reflected from a corner cube mounted on a computer controlled motorized delay line which provides the time delay between the two pulses. The two beams are crossed at ~1° angle in the sample, which is located in a liquid He cryostat. The temperature can be varied from 1.5 to 15 K. The echo pulse is directed into a phototube whose output is processed with a lock-in amplifier. The echo intensity and a voltage corresponding to the time delay are digitized by the computer and stored. Since the instrument response is 30 ps and typical decays are on the order of 1 ns, the data can be simply fit to an exponential decay without convolving the instrument response function. The experiments were performed on low concentration [1×10^{-6} mole guest/mole host (M/M)] samples to avoid effects arising from guest–guest interactions[18] and at low powers to avoid optical density effects.[19] The decay constant is plotted as a function of temperature, yielding the temperature dependence of the dephasing time.

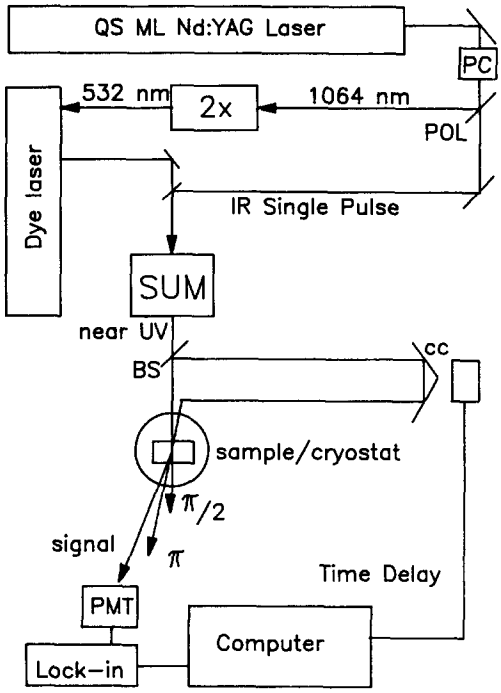

FIG. 1. Experimental configuration for the picosecond photon echo experiment. The Pockels cell (PC) and polarizer (POL) select an IR single pulse which is summed with the cavity dumped output of the dye laser. The generated near-UV beam can be tuned from ~365–415 nm. BS = beamsplitter; CC = corner cube on motorized delay line; PMT = photomultiplier tube.

Linear absorption spectroscopy of the samples was performed using a Xe arc lamp through a 3/4 m monochromator with 6 μm slits, yielding 0.5 cm^{-1} resolution. The light was polarized using a sheet polarizer and weakly focused onto the sample. The light was collected by a phototube and digitized, as was the wavelength.

Fluorescence lifetimes were measured at 1 K by exciting the chromophore in the phonon side band of S_1 and monitoring the fluorescence from S_1 to either the S_0 zero-phonon line, the 390 cm^{-1} vibrational line, or the 1400 cm^{-1} vibrational line. Fluorescence was detected with a multichannel plate and digitized by a transient digitizer. It was fit by convolving the instrument response of the transient digitizer with an exponential decay.

The phenanthrene was prepared by reacting 98% pure phenanthrene twice with maleic anhydride to remove anthracene.[20] Anthracene is the principal naturally occurring impurity in phenanthrene (it is the other 2%) and does not zone refine out because of a segregation coefficient close to unity.[20] The anthracene-free phenanthrene was then zone refined for >200 passes and the center sections were used. Absorption spectra of these sections revealed less than 10 ppb of anthracene. The anthracene guest was zone refined Kodak X480 stock. The methyl-substituted anthracenes were 99% pure from Aldrich and were sublimed twice before use. Boules of each guest/host system were grown with concentrations from 5×10^{-7} to 5×10^{-6} M/M using standard Bridgman methods.

The boules cleaved nicely in the *ab* plane and crystals were mounted with the *b* axis parallel to the laser polarization. The transitions of the guests were experimentally determined to be *b* axis polarized. The cleaved crystals exhibited striations parallel to the *b* axis, but were of acceptable optical quality. These striations became apparent after the crystal slowly cooled through the phase transition at 72 °C.[21,22]

III. EXPERIMENTAL RESULTS

Figure 2 displays guest absorption spectra of the three systems. All are characterized by a broad inhomogeneous line with a large featureless phonon sideband. For anthracene, the zero-phonon line (ZPL) has a FWHM of 20 cm^{-1}, calculated by measuring the HWHM on the red side of the line and doubling its value. This avoids the ambiguity introduced by the phonon sideband. The distance between the peak of the ZPL at 3832.9 Å and the peak of the phonon sideband (PSB) is 28 cm^{-1}. In the case of 9-methylanthracene, the ZPL occurs at 3978.6 Å, has a FWHM of 14 cm^{-1} and is separated from the peak in the PSB by 29 cm^{-1}. For 2-methylanthracene, the ZPL at 3908.3 Å has a FWHM of 15 cm^{-1} and the distance to the peak of the PSB is 26 cm^{-1}. These wavelengths are not vacuum corrected. All spectra presented were recorded between 1–1.5 K. The concentrations used for the spectra varied from 2×10^{-6} M/M for the 9-methylanthracene to 5×10^{-6} M/M for anthracene. The observed ODs are not directly related to the concentrations because the crystals were of different thicknesses. The formula used for calculating the guest concentrations is (in cgs units):

$$C\,(\mathrm{M/M}) = \frac{\hbar V_{uc} n_b^3 \lambda\, \mathrm{OD}_{max}\, \mathrm{FWHM}}{8\pi N_{uc}\mu^2 \cos^2\theta\, \mathrm{TH}}, \qquad (1)$$

where C is the concentration of the guest in units of mole/mole (M/M), $\hbar$ is Planck's constant, V_{uc} is the volume of the phenanthrene unit cell and N_{uc} is the number of molecules per unit cell (two for this case), n_b is the index of refraction of phenanthrene, μ is the anthracene transition dipole moment with cos θ the angle between the dipole moment and the *b* axis,[23] OD_{max} is the optical density at the peak absorption wavelength λ, FWHM is the inhomogeneous full-width at half-maximum, and TH is the thickness of the sample. The constant coefficients in this formula differ from those reported previously[24] because the inhomogeneous lines for these systems are fit better by a Lorentzian line shape than by a Gaussian line shape. For a Gaussian line shape, the factor of 1/8 is replaced by 0.195.

In these samples, the inhomogeneous linewidth is broader than that of many other mixed crystal systems by about a factor of 10.[15] There are three factors which could contribute to this extra broadening, all of which stem from the structure of the phenanthrene molecule and are related to the phase transition at 72 °C. Repulsion between the 4 and 5 hydrogens of phenanthrene (see Fig. 5) tends to place them on opposite sides of the central ring, giving the molecule roughly C_2 symmetry in the low temperature phase, although lattice packing distortions cause the molecules to have C_1 symmetry.[25] The symmetry ensures that phenanthrene has a small dipole moment. In the high temperature phase, both hydrogens can be on the same side of the phenanthrene molecule.[21,26] This configuration might exist

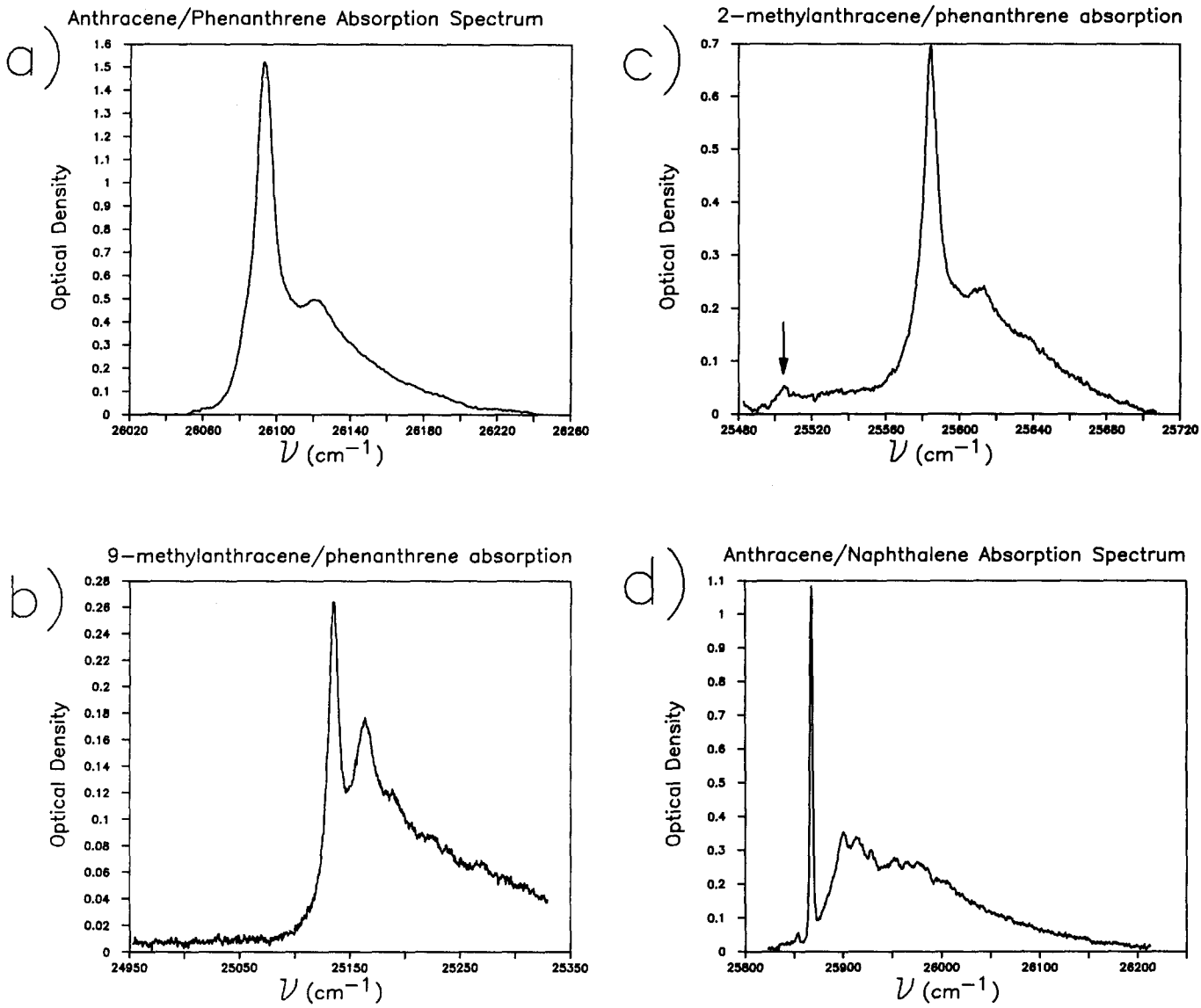

FIG. 2. Absorption spectra of systems under consideration. (a) anthracene/phenanthrene. The peak of the ZPL is at 3832.9 Å and distance to the peak in the PSB is 28 cm^{-1}. The inhomogeneous FWHM is 20 cm^{-1}. (b) 9-methylanthracene/phenanthrene. The ZPL is at 3978.6 Å, has a width of 14 cm^{-1}, and the distance to the PSB peak is 29 cm^{-1}. (c) 2-methylanthracene/phenanthrene. The ZPL is at 3908.3 Å, has a width of 15 cm^{-1}, and the distance to the PSB is 26 cm^{-1}. There is a minor peak in the spectrum at 3919.6 Å which is another monomer origin (see the text). (d) anthracene/naphthalene. The ZPL is at 3865.4 Å, has a width of 3.6 cm^{-1}, and there is a noticeable peak in the PSB 34 cm^{-1} to the blue of the ZPL.

around the guest at low temperatures due to local distortions in the potential caused by the guest. In the low temperature guest/host system, the phenanthrene molecules surrounding each guest molecule will be random mixtures of the various permissible conformers, so the guests will experience a wide variety of local environments. Since the electronic transition energy of the guest is sensitive to the structure of the local environment, the structural disorder of the 4,5 hydrogens of the host molecules causes inhomogeneous broadening. Any dipole field of the disordered environment will cause further broadening. In addition, there will also be broadening due to the residual strain in the crystal resulting from the phase transition.

These spectra can be contrasted to the absorption spectrum of 2×10^{-7} M/M anthracene in naphthalene displayed in Fig. 2(d). The distance between the ZPL at 3865.4 Å and the PSB is 34 cm^{-1} and agrees well with the fluorescence spectrum of the anthracene/naphthalene system.[27] In this system, the FWHM of the inhomogeneous line is 3.6 cm^{-1}. Naphthalene does not have a variety of possible hydrogen structures, nor does it possess a dipole moment. Furthermore, naphthalene does not undergo a phase transition. Thus, the inhomogeneous broadening in the phenanthrene systems can be attributed to the local structure of the host.

The large phonon sideband in these systems is evidence of strong linear mixing of the anthracene guest excitation with the host acoustic phonon modes. In the systems discussed here, the Debye–Waller factor is about unity, which is large compared to other systems of this type.[14,15] The large linear excitation-phonon coupling suggests the possibility that quadratic coupling to the acoustic phonons could also be large in these systems, as has been observed in diazaazulene/naphthalene.[9,28] The photon echo experiments can determine if quadratic coupling to acoustic phonons, optical

phonons, or to a pseudolocal phonon is dominant and is responsible for optical dephasing.

In the photon echo experiment, the measured dephasing rate is the sum of two rates: the rate at 0 K due to the excited state lifetime and the temperature dependent (pure dephasing) rate. They are related by the following formula[13]:

$$1/T_2 = 1/T_2^* + 1/2T_1, \tag{2}$$

where $1/T_2$ is the measured echo decay rate, $1/T_2^*$ is the temperature dependent decay rate, and T_1 is the excited state lifetime which is measured by the decay of fluorescence. T_1 values for the three systems studied are given in Table I.

The dephasing caused by quadratic coupling to a pseudolocal phonon mode has an Arrhenius temperature dependence at low temperatures of the form[9]

$$1/T_2^* = 1/T_2^*(\infty)\exp(-E/kT), \tag{3}$$

where E is the activation energy, k is Boltzmann's constant, and $T_2^*(\infty)$ is a prefactor related to the lifetime of the pseudolocal mode. The model of a pseudolocal mode views it as a single energy level with Lorentzian broadening because of the lifetime of the mode. The lifetime (decay of motion) and excitation of the mode occurs because of weak coupling to acoustic phonons.

Optical dephasing via quadratic coupling to acoustic phonons at low temperature gives a T^7 temperature dependence, i.e.,

$$1/T_2^* = A(T/T_D)^7, \tag{4}$$

where T_D is the Debye temperature and A is a constant depending on the coupling strength and the Debye temperature.[9]

Quadratic coupling to optical phonons yields a temperature dependence which is a function of the form of the phonon density of states. For a hemispherical density of states,[29] for example,

$$1/T_2^* = F\sinh[\hbar\Gamma_B/2kT]\exp[-E/kT], \tag{5}$$

where Γ_B is the bandwidth of the optical phonon, E is its energy, and F is a constant depending on the bandwidth, energy, and coupling strength. While this is not strictly an exponentially activated process it is difficult to distinguish it from one in the presence of experimental noise.

Figure 3 displays two typical photon echo decays of anthracene/phenanthrene and their exponential fits. In curve (a), the echo was recorded at a temperature of 3.83 K, where the pseudolocal dephasing mode is not appreciably thermally activated. The measured decay constant of 12.2 ns is twice the fluorescence lifetime of 6.0 ns, within experimental error. In curve (b), the echo decay was recorded at 5.88 K. It is evident from its 4.2 ns decay constant that phonon induced dephasing is beginning to play a role. As the temperature is increased further, the dephasing rate increases rapidly.

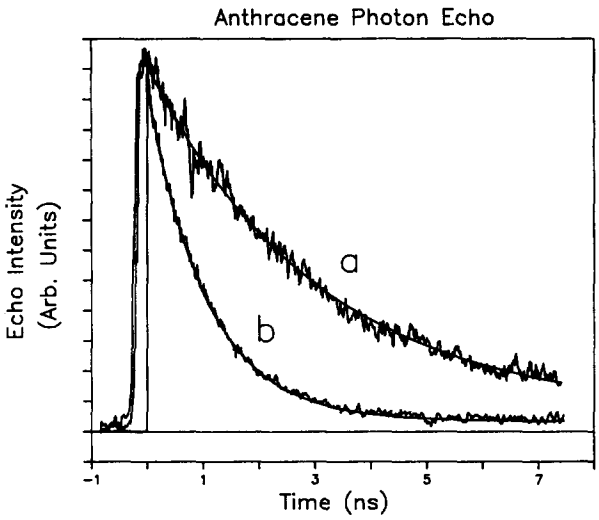

FIG. 3. Example of photon echo decays for the anthracene/phenanthrene system with single exponential fits. (a) The temperature $T = 3.83$ K and the observed $T_2 = 12.2$ ns. At this temperature $T_2 = 2T_1$, and lifetime effects dominate the optical dephasing. (b) $T = 5.83$ K and the observed $T_2 = 4.2$ ns, showing that phonon induced dephasing is beginning to play an important role.

In Fig. 4 the natural logarithm of T_2^* is plotted as a function of $1/T$ for the three systems along with a best fit line for each. A good fit to a straight line indicates an Arrhenius activation process. Table I summarizes the results for the three systems. The first column is the fluorescence lifetime of the sample, the second columm is the activation energy of the pseudolocal mode from the slope of the plot in Fig. 4, and the third column is the prefactor $T_2^*(\infty)$.

The fact that the dephasing in all three cases has an Arrhenius temperature dependence eliminates coupling to

TABLE I. Experimental parameters for pseudolocal mode dephasing in anthracene and 9- and 2-methylanthracene in phenanthrene.

Guest	T_1 (ns)	E (cm^{-1})	$T_2^*(\infty)$ (ps)
Anthracene	6.0 ± 0.1	28.4 ± 0.5	5.8 ± 0.5
9-Methylanthracene	5.8 ± 0.1	23.7 ± 0.5	7.4 ± 0.5
2-Methylanthracene	7.0 ± 0.1	28.5 ± 0.5	3.0 ± 0.5

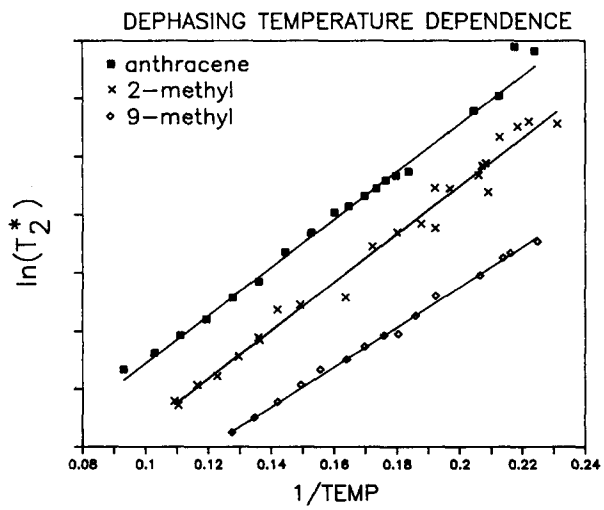

FIG. 4. Temperature dependence of the pure dephasing rate for the three systems studied. All three systems are fit well by an Arrhenius temperature dependence. The numerical results are tabulated in Table I. The form of the temperature dependence eliminates quadratic coupling to acoustic phonons as the dephasing mechanism.

acoustic phonons as the dephasing mechanism in the temperature range studied. The fact that the activation energy of 9-methylanthracene is significantly different from that of anthracene or 2-methylanthracene eliminates coupling to an optical phonon as the dephasing mechanism. This is because the optical phonon frequency is a property of the host material, and does not change for different guest molecules. Quadratic coupling to an optical phonon would give the same temperature dependence for all three guests, in contrast to what is observed. In addition, the nearest measured optical phonon frequency of phenanthrene is 31 ± 1 cm^{-1}.[30] Thus, we conclude that a pseudolocal mode is responsible for dephasing in each of the three systems.

In the simple picture of pseudolocal mode dephasing, one would conclude that 2-methylanthracene, with its larger mass and moments of inertia, would have a lower pseudolocal mode energy than anthracene. The fact that this is not the case implies that the structure of the host around the chromophore strongly influences the local dynamics of the guest. The computer simulations of the local structure and normal modes were performed with the objective of understanding the experimentally observed activation energies and to examine the librational and translational character of the local modes.

IV. DESCRIPTION OF CALCULATIONS

The local motions of each of the three guests were simulated by constructing a small phenanthrene crystal containing a guest molecule, minimizing the crystal's energy, and performing a normal mode analysis. Crystals of two different sizes were studied: $2\times3\times2$ unit cells and $3\times4\times3$ unit cells, comprising 24 and 72 molecules, respectively. This allows system size effects to be studied. All molecules were treated as rigid bodies, except methyl group rotation was allowed. A rigid body approximation is suitable because the lattice modes of interest, typically 30 cm^{-1}, are much lower than the lowest intramolecular modes of these molecules. The lowest internal mode of phenanthrene is $\sim$229–234 cm^{-1} (Ref. 30) and that of anthracene is $\sim$100 cm^{-1}.[31] Methyl group librations typically lie in the 100–200 cm^{-1} range.[32]

Atomic coordinates and unit cell constants for phenanthrene were taken from room temperature diffraction data.[33] A planar anthracene guest was constructed from crystal structure data at 95 K.[34] A methyl group was constructed with a carbon at the center of a tetrahedron, hydrogens at three vertices ($d_{C\text{-}H} = 1.11$ Å), and the 1.51 Å C–C bond of attachment[35] directed to the fourth vertex. The methylated guests were constructed by removing the appropriate H atom from the anthracene and placing the methyl group carbon on the intersection of the anthracene plane and the plane bisecting a line joining the two anthracene ring hydrogens nearest the methyl group.

Once the replicated host unit cells were built, a single phenanthrene was replaced by the guest molecule. The guest was oriented so that its long, short, and out-of-plane axes matched those of the displaced host and was located so that their centers of mass coincided. Because of the C_1 site symmetry of the phenanthrene crystal, there are two such orientations for a 9-methylanthracene guest and four such orientations for a 2-methylanthracene guest. These can be conveniently considered to be 9- and 10-methylanthracene, and 2-, 3-, 6-, and 7-methylanthracene molecules. Figure 5 depicts a phenanthrene unit cell containing an anthracene guest with the six possible methyl group substitution positions identified.

The interaction energy of the guest-containing crystal is the sum of all intermolecular atom pair interactions out to a cutoff distance of 10 Å for the $3\times4\times3$ system and 8 Å for the $2\times3\times2$ system. Periodic boundary conditions were employed, and system dimensions were always at least twice the cutoff distance so only minimum-image interactions needed to be considered. Although the methyl-to-anthracene intramolecular interactions were used in energy minimization, the lattice energies reported here exclude these terms, i.e., they are purely intermolecular energies.

An extensively modified version of the program WMIN[36] was used to perform the calculations. The atom pair interaction is a Buckingham (6-exp) potential function using Williams' parameter set IV.[37] The total interaction energy of a complete guest/host system was minimized by adjusting all molecular positions and orientations, the lengths of the sides of the system, and if present, the methyl group rotation angle. The cell angles were held constant although it is not expected that varying β, to maintain monoclinic symmetry, would alter the results. Standard minimization techniques were used: conjugate gradient minimization, followed by steepest descents minimization, and finally Newton–Raphson minimization. Each molecule was allowed to translate along and rotate about its principal moment axes. Guest rotation was always about the molecular center of mass and methyl group rotation was about the C–C bond joining it to the body of the guest.

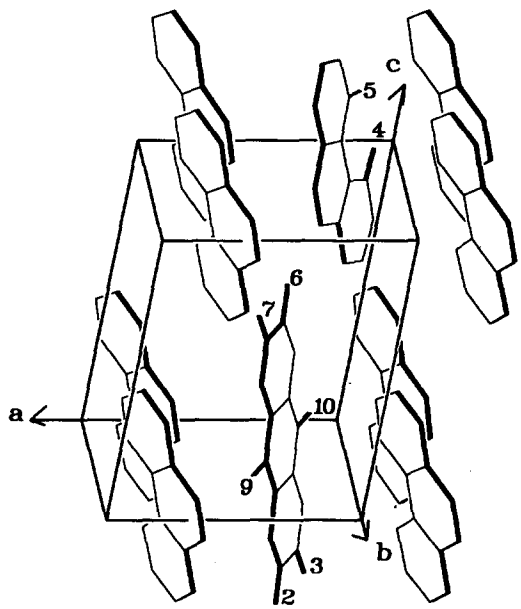

FIG. 5. Orientation of an anthracene guest in a phenanthrene lattice with methyl substitution positions and crystallographic axes labeled. The locations of hydrogens 4 and 5 on one of the phenanthrene molecules is also indicated.

TABLE II. Lowest energy local mode results for 3×4×3 unit cell system (72 molecules, r_{cut} = 10 Å, step sizes 2° and 0.1 Å).

Crystal	E_{lat} (kcal/mol)	Freq. (cm^{-1})	Lib. axis			Trans. axis			Motion(deg/Å)		
			L	*M*	*N*	*L*	*M*	*N*	ρ_c	ρ_e	ρ_c/ρ_e
phen	−1656.72										
A/*P*	phen + 0.82	44	−0.05	0.25	0.97	0.99	0.11	0.02	20.9	4.4	4.7
9-*A*/*P*	phen + 2.76	37	−0.03	0.02	−1.00	0.96	0.27	−0.02	20.6	25.1	0.82
10-*A*/*P*	phen + 6.51	39	−0.08	0.14	0.99	0.99	0.10	0.03	20.7	20.9	0.99
2-*A*/*P*	phen + 5.36	46	−0.08	0.05	−1.00	0.99	0.10	0.08	19.2	8.7	2.2
3-*A*/*P*	phen + 3.97	48	−0.60	−0.13	0.79	0.95	0.31	−0.01	22.8	7.7	3.0
6-*A*/*P*	phen + 2.73	42	−0.06	0.16	0.99	0.99	−0.12	0.02	19.2	7.2	2.7
7-*A*/*P*	phen + 5.21	46	−0.87	−0.19	−0.45	0.98	0.20	0.04	31.5	1.0	31.1

As a preliminary step, the guest was fully relaxed in its site before the host molecules and system sides were freed. Thereafter full minimization of the entire system was performed until the root sum of the squares of the gradient amplitudes of all translational or librational structural parameters was less than 5×10^{-5} kcal/mol Å or 5×10^{-5} kcal/mol radian, and energy fluctuations between minimization cycles were less than 10^{-7} kcal/mol. After minimization, the molecular geometries were checked to ensure that no distortions had occurred during minimization. Internal coordinate changes were found to be less than 1×10^{-10} Å.

For each of the systems, a normal mode analysis[38] was performed in which the guest was free to move in the lattice of relaxed frozen host molecules. The analysis requires a matrix of second derivatives of lattice potential energy with respect to changes in the molecular degrees of freedom, which is obtained by finite difference techniques. In an anharmonic system this matrix and the resultant frequencies and normal modes would depend on the parameter step size and the degrees of freedom used to calculate the second derivatives. In a harmonic system this dependence would be absent. To study the amount of anharmonicity, normal mode analyses were performed for a variety of step sizes in the allowed degrees of freedom (translations along and rotations about three mutually orthogonal directions). These ranged from very small (10^{-4} Å and 0.005°) to twice the typical classical turning-point values for these systems (~0.1 Å and ~2°). In addition, three different basis sets of translation and rotation axes were used: the molecular principal moment axes; the molecular short, long, and out-of-plane axes; and the crystal *a*, *b*, and *c** axes.

V. RESULTS OF CALCULATIONS

Results of the calculations for phenanthrene, anthracene, and each of the orientations of 9-methylanthracene and 2-methylanthracene are presented in Table II (3×4×3 case) and Table III (2×3×2 case). The methyl-substituted anthracene guests are denoted by *n*-*A*/*P*, where *n* is the anthracene carbon atom to which the methyl group is attached (see Fig. 5). The tables give the total lattice energy of each system studied, the frequency of the lowest energy normal mode (calculated with a frozen host lattice), and descriptive information about this mode.

The pure phenanthrene lattice energy in the two tables, divided by the number of molecules in the sample, is −23.01 and −21.75 kcal/mol, respectively. These are very close to the observed phenanthrene sublimation enthalpy of 21.63 kcal/mol.[39] The larger system differs more because it uses a 10 Å cutoff and the potential parameters used were developed for 8 Å.[37] The phenanthrene lattice energy for the larger system using an 8 Å cutoff is −1567.93 kcal/mol, or −21.77 kcal/mol per molecule.

Each of the guest-containing systems has a higher lattice energy than that of pure phenanthrene. Anthracene causes by far the least change in lattice energy—strong evidence that a methyl group creates substantial local lattice distortion.

TABLE. III. Lowest energy local mode results for 2×3×2 unit cell system (24 molecules, r_{cut} = 8 Å, step size 2° and 0.1 Å).

Crystal	E_{lat} (kcal/mol)	Freq. (cm^{-1})	Lib. axis			Trans. axis			Motion(deg/Å)		
			L	*M*	*N*	*L*	*M*	*N*	ρ_c	ρ_e	ρ_c/ρ_e
phen	−522.07										
A/*P*	phen + 0.29	42	0.01	0.34	0.94	0.99	0.10	0.02	20.9	4.6	4.5
9-*A*/*P*	phen + 2.29	34	−0.03	0.01	−1.00	0.97	0.26	−0.03	20.6	27.3	0.76
10-*A*/*P*	phen + 6.28	37	−0.06	0.18	0.98	1.00	0.08	0.04	20.8	21.7	0.96
2-*A*/*P*	phen + 5.27	44	0.02	0.10	−0.99	0.91	0.41	0.08	19.1	14.7	1.3
3-*A*/*P*	phen + 3.02	46	−0.63	−0.17	0.76	0.96	0.29	−0.01	23.3	7.2	3.2
6-*A*/*P*	phen + 1.88	39	0.04	0.29	0.96	1.00	−0.07	0.02	19.3	6.8	2.8
7-*A*/*P*	phen + 3.97	44	0.11	0.14	−0.98	0.90	0.43	0.04	19.2	4.5	4.3

The two different 9-methylanthracene orientations differ in energy by 3.75–3.99 kcal/mol. If this energy difference were maintained at the 101 K melting point of phenanthrene, one would expect the population ratio of the two orientations to be greater than 150:1. Thus, if the lattice energies are at all meaningful, the 10-methylanthracene orientation can be ignored.

The four different 2-methylanthracene orientations differ by a similarly wide range of energies. The lowest energy orientation, 6-methylanthracene, differs in energy from that of the next lowest, 3-methylanthracene, by 1.14–1.24 kcal/mol. At 101 K this would result in a population ratio of about 5:1 for the two orientations. Thus, the 6-methylanthracene orientation of 2-methylanthracene is probably the one upon which the experiments were performed.

Tables II and III also present the frequencies of the lowest energy normal mode calculated for each system in the frozen host lattice approximation, using step sizes of 0.1 Å and 2°, and using the short, long, and out-of-plane axes (standard LMN axes) of the anthracene part of each guest as a basis. For step sizes smaller than these, regardless of the translation and rotation axes used, the calculated frequencies remained essentially unchanged. Only at twice these step sizes did the calculated frequencies differ by more than 1 cm^{-1} from the values in the tables. Thus, the rigid lattice potentials in which the guest molecules move are very close to quadratic for physically reasonable choices of the step size, and the frequencies in the tables have error bars of about 1 cm^{-1}.

The most important observation to be made about the calculated frequencies is that those for the 9-methylanthracene orientations are less than those for either anthracene or the 2-methylanthracene orientations. If one considers just the energetically most likely orientations of the methylated guests, the local mode frequencies for anthracene and 6-methylanthracene are about equal and that for 9-methylanthracene is about 5–6 cm^{-1}, or ~15%, less. *This trend and its magnitude is the same as that observed experimentally. The ratios of the experimental frequencies are almost the same as the ratios of the calculated frequencies.*

The frequencies calculated for the $2\times3\times2$ system are uniformly lower than those for the $3\times4\times3$ system by 2–3 cm^{-1}. This is not due to the different potential cutoff distances used, because the frequencies of the larger system remain unchanged if an 8 Å cutoff is used. Evidently the larger system is slightly better able to pack around the guest molecule, resulting in higher frequencies.

Unlike earlier local mode calculations,[16] the guest molecule in these calculations was allowed both librational and translational degrees of freedom. The eigenvectors of the resulting normal modes have three librational and three translational components. The mode associated with motion of the methyl group is well separated in energy from the lower modes and will not be considered further. The translational components form a three vector giving a direction and a relative magnitude (in Å) of translation of the normal mode. Similarly, the three librational components describe a rotation matrix which is expressible as a direction vector and a relative magnitude (in degrees) of libration about that vector. Normalized libration and translation axes for the lowest energy normal mode of each guest relative to its LMN axes are presented in Tables II and III.

The ratio of the magnitudes of the librational and translational components of the eigenvector ρ_e provides a direct measure (in degrees/Å) of the relative amounts of each type of motion present in the local mode. This ratio can be interpreted in the following way. The classical turning point amplitude of a purely translational harmonic oscillator is given by

$$x=\left[\frac{(n+1/2)\hbar}{\pi c\nu m}\right]^{1/2}, \tag{6}$$

where n is the principal quantum number, ν is the transition energy in cm^{-1}, and m is the molecular mass. For a purely librational mode, the classical turning point amplitude θ is given by an identical expression, except m is replaced by the moment of inertia I about the libration axis. Typical values for a $\Delta n=1$ change in x and θ are 0.1 Å and 2°, respectively. The ratio of these two classical turning point quantities, $\rho_c=\theta/x=\sqrt{(m/I)}$, depends only on the molecular mass and the moment of inertia. If the motion of the pseudolocal mode were equally partitioned between librational and translational degrees of freedom, then its libration/translation amplitude ratio would equal ρ_c. Comparing this ratio to that calculated from the lowest mode's eigenvector ρ_e one can characterize the normal mode as mostly librational if $\rho_c \ll \rho_e$, mostly translational if $\rho_c \gg \rho_e$, or a mixture of both.

Tables II and III also contain values of ρ_c, ρ_e, and ρ_c/ρ_e for each of the systems studied. For the lowest energy orientation of each guest, ρ_c and ρ_e did not vary by more than 2°/Å for all step sizes up to 4° and 0.2 Å.

The ρ_c/ρ_e values in the tables indicate that the anthracene local motion is largely translational, the motion of the two 9-methylanthracene orientations is about an equal mixture of translation and libration, and the motion of the four 2-methylanthracene orientations is mostly translational, but with more librational character than anthracene. For each of the guest types and orientations, translation occurs approximately along the long molecular axis and, generally, the libration occurs about the out-of-plane molecular axis.

It should be mentioned that the calculations produce six (or seven if the methyl motion is included) local modes for each guest. Only the lowest mode contributes to dephasing, because in each case the next lowest mode is 7–14 cm^{-1} higher in energy and is relatively unpopulated over the experimental temperature range. Analysis of the higher energy modes indicates that, with the exception of the methyl libration, they too are combinations of translational and librational motion. The energy of the methyl group libration is greater than 300 cm^{-1}, well above the other modes, and its motion does not contribute significantly to the lower energy modes.

It is interesting to note that, when only librational degrees of freedom were permitted, the lowest-mode frequencies increased an average of 18 cm^{-1} but the two 9-methylanthracene orientations remained substantially lower in frequency than the other guests. The libration axis was always within 20° of the out-of-plane molecular axis. When

TABLE IV. Unit cell constant and volume changes upon energy relaxation (units are Å and Å^3).

Crystal	2×3×2 unit cell system a	b	c	Avg. vol.	3×4×3 unit cell system a	b	c	Avg. vol.
phen	8.058	6.050	9.659	466.3	8.018	6.049	9.636	462.8
A/P	8.035	6.049	9.693	466.6	8.013	6.047	9.648	462.9
9-*A/P*	8.128	6.037	9.669	469.8	8.044	6.043	9.640	464.0
10-*A/P*	8.160	6.031	9.678	471.6	8.049	6.046	9.641	464.6
2-*A/P*	8.031	6.070	9.771	471.1	8.010	6.059	9.664	464.4
3-*A/P*	8.047	6.046	9.773	470.9	8.017	6.047	9.673	464.4
6-*A/P*	8.077	6.049	9.702	469.4	8.032	6.044	9.651	463.9
7-*A/P*	8.019	6.076	9.764	471.1	8.008	6.058	9.669	464.5

only translational motion was permitted, the frequencies of the two 9-methylanthracene orientations were no longer significantly lower than those of the other guests, although the translations were all very well aligned with the guest's long molecular axis. Thus, although there appears to be a significant amount of translational character in the local motions, it is the strong admixture of librational motion which is responsible for the lower frequency of 9-methylanthracene.

The initial unit cell constants used for all the guests were $a = 8.472$ Å, $b = 6.166$ Å, and $c = 9.467$ Å which yields a unit cell volume of 489.7 Å for $\beta = 98.01°$.[3] The cell constants and average cell volumes of each of the relaxed systems are given in Table IV. The numbers in the table are the length of the side (or the volume) of the final system divided by the nominal number of cells along the side (or in the volume). Several interesting points can be made. First, all of the calculated systems relax to a longer *c* axis and shorter *a*- and *b*-axis values. This is a result of the potential, which was not optimized for phenanthrene. Second, the average cell volume of each of the guest containing systems is larger than that of pure phenanthrene. Anthracene causes only a very small expansion, but the methylanthracenes cause an average volume expansion of about 0.3% for the 3×4×3 systems and 0.9% for the 2×3×2 systems. For each guest, the average volume change is less for the larger system, since the guest's effect is averaged over more unit cells. The total volume change is the same for the two system sizes. The fully relaxed systems (effectively at 0 K) have cell volumes 3.7%–5.5% smaller than the room-temperature experimental value.

In pure phenanthrene, the long molecular axis is approximately aligned with the crystalline *c* axis and the out-of-plane axis lies in roughly the *ab* plane. When anthracene is substituted, there is very little change in the cell constants. When 9-methylanthracene is substituted, because the methyl group lies approximately in the *ab* plane (see Fig. 6), the *c* axis is little changed. In this case, the *a* axis lengthens and the *b* axis contracts, despite the fact that the C–C bond to the methyl group, when projected onto the *ab* plane, makes only a 28° angle with the *b* axis. For the four 2-methylanthracene orientations, the methyl group significantly lengthens the molecule, so the crystal's *c* axis lengthens considerably and the *a* and *b* axes are only slightly altered. This can be understood by examining Fig. 7, which shows the methyl group of 6-methylanthracene protruding into the interstitial space between *ab* layers of molecules.

One further important point should be made. When energy relaxation was performed on the systems studied with the unit cell constants held at the crystallographic values,[33] it was found that all the guests exhibited similar normal mode frequencies. Thus, although the cell constants change by very little, it is necessary to allow them to vary so that the host can accommodate guests of different shapes and sizes.

VI. DISCUSSION

In both the experimental and calculated results, anthracene and 2-methylanthracene exhibit the same pseudolocal mode energies while 9-methylanthracene has a significantly lower one. Although the calculated energies are ~50% larger than the experimental ones, both the trend and its magnitude are reproduced. The 9-methylanthracene energy is about 84% that of the other two guests in both cases. The agreement of the relative energies supports the idea that the calculated eigenvalues are a good representation of the natural modes of the system. The major characteristic of the lowest energy normal mode in all three systems is that it is a combination of translational and librational motion. The translation occurs along the long axis of the guest, while the libration is about the out-of-plane axis.

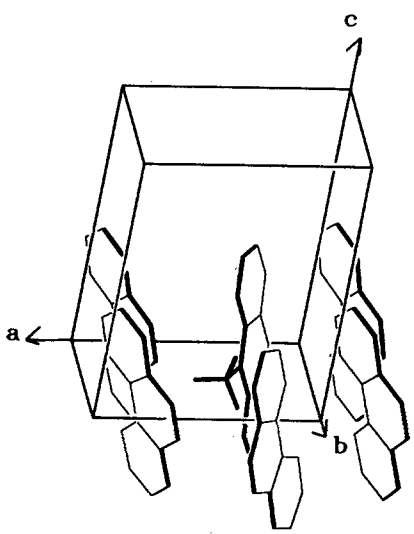

FIG. 6. Orientation of 9-methylanthracene in phenanthrene. The methyl group lies between two host molecules. This position hinders its translational motion, which could account for the enhanced librational character of the pseudolocal mode.

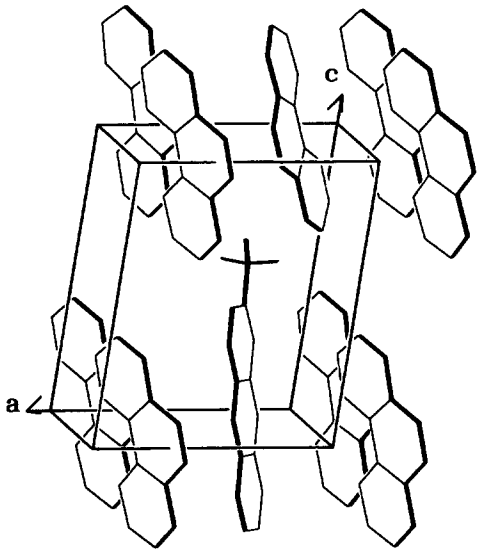

FIG. 7. Orientation of 6-methylanthracene in phenanthrene. The methyl group lies in the interstitial space between layers of molecules in the *ab* plane.

The motion of anthracene is predominantly translational, with only a small amount of librational motion. The 2-methylanthracene system is also largely translational, but has a greater librational contribution. This is probably due to interactions of the bulky methyl group with phenanthrene molecules in the neighboring *ab* place (see Fig. 7). In contrast to the other two guests, 9-methylanthracene has more librational than translational character, although they are nearly balanced. As Fig. 6 shows, the methyl group in this system is directed between two host phenanthrene molecules. Apparently it is locked in place, making translation difficult and the pseudolocal mode more librational.

There is additional evidence supporting the assignment of mixed librational and translational character to the pseudolocal mode. Recent lattice dynamic calculations by Kulver and Eckhardt[26] of the optical modes of pure phenanthrene assign the lowest energy optical phonon to a purely translational motion at 19 cm^{-1}, and the second lowest one to a purely librational motion with an energy of 36 cm^{-1}. The motion for the translational mode is primarily along the c^* axis, with some motion along the *a* axis. This direction is roughly aligned with the long molecular axis of the molecules. The motion for the librational mode is about the *b* axis of the crystal. The energies of these two modes bracket our experimentally measured energies. Thus, it is reasonable to expect that the pseudolocal motions of the guests in the systems studied here would be similar. However, it is still necessary to perform the normal mode analysis to obtain the details of the pseudolocal eigenvectors.

The experimentally determined energies of the pseudolocal modes are also located within the acoustic phonon bands of the host. One might expect that the translational component of a pseudolocal mode would mix well with the acoustic phonons leading to a correlation between the amount of translational motion and the lifetime of the mode. The amount of translational motion is given by the ρ_c/ρ_e values in Tables II and III. However, the $T_2^*(\infty)$ values in Table I, while related to the pseudolocal mode lifetimes, also depend on the excitation-phonon quadratic coupling strength, which is not necessarily the same for all three systems.[9] Therefore, although such a correlation might exist, it cannot be verified. One might also expect that modes that are largely translational, with energies that lie in the acoustic phonon band, would be delocalized. Generally, any perturbation of the local potential is sufficient to cause some localization,[40] the degree of which depends on the magnitude of the perturbation. Even in an atomic system, where only translational motions can occur, a sufficiently different impurity will result in a localized translational mode. So there is no *a priori* reason to expect translational motion of a guest to be delocalized.

The discrepancies between the calculated and the observed energies are due in large part to the frozen lattice approximation. In a pseudolocal mode the guest contains much of the energy in the mode, but some resides in the host. One can visualize the energy density of the mode as decaying away spatially from the guest, implying that the nearby neighbors of the guest move slightly. In the calculations discussed here, all the molecules of the host were fixed. This increases the repulsive forces felt by the guest as it moves away from the energy minimum, raising its pseudolocal mode frequency. If the calculations were performed in a manner which allowed the neighboring host molecules to move, the pseudolocal energy of the mode should decrease. This would bring the calculated mode energies closer to the observed values. However, since the motion is mostly localized on the guest, the calculated frozen host eigenmodes should provide a good representation of the system's behavior.

The calculated eigenvalues and eigenvectors could be improved by altering the potential function. Lattice dynamics calculations are generally improved by adding Coulombic or multipolar terms to the potential.[41] In addition, the parameter set was developed for room temperature polycyclic aromatics, using an 8 Å cutoff, and all C–H bonds 1.027 Å in length.

In the 2-methylanthracene system, there are four possible orientations of the guest in the lattice. This should lead to four different origins. However, the different orientations have different site energies and will not be populated equally. This is observed experimentally. In samples with a high concentration of 2-methylanthracene, about 10^{-5} M/M, one can see different transitions in the spectrum, such as that shown in Fig. 2(c) at 25 513 cm^{-1}, $\sim$80 cm^{-1} to the red of the dominant spectral feature. By measuring the OD as a function of concentration, it was determined that this transition is monomeric, and not due to dimer formation in the crystal. By measuring the relative peak areas, and assuming that the two sites are Boltzmann populated at the melting point of the phenanthrene crystal, 374 K, the difference in the site energies can be estimated. In Fig. 2(c) the ratio of the peak areas is $\sim$10:1, which implies a site energy difference of 1.7 kcal/mol. The calculated difference in site energy between 6-methylanthracene and 3-methylanthracene is 1.2 kcal/mol, which is within 50% of the observed value. This is

further evidence that, although the potential function could be improved, it is capable of providing detailed insights into this problem.

In the 9-methylanthracene system, there are two possible guest orientations, but only one origin is observed experimentally. This could be due to a site energy difference which is so large that the second site is not appreciably populated, or the second site is populated to a small extent but its ZPL is buried in the absorption of the dominant site. In general, the electronic transition energy of a guest is not correlated with its site energy. However, the calculated site energy difference of 3.75 kcal/mol for this system would result in a population ratio of $\sim 150{:}1$, which would not be observable in an absorption spectrum.

VII. CONCLUSIONS

The motion responsible for dephasing in the mixed crystal systems anthracene/phenanthrene, 9-methylanthracene/phenanthrene, and 2-methylanthracene/phenanthrene is a mixture of translational and librational local motions. The translation is predominantly along the long axis of the guest, while the libration is about the out-of-plane axis. It is to be expected that similar results would apply to other condensed phase systems. The important influence of the local structure around the guest on the pseudolocal mode energy has been discussed. Although the calculated energies do not match the observed values absolutely, the ratios are all consistent. Improvements could be made to the potential function that was used. Relaxing the frozen lattice approximation to allow motion of the nearest neighbors would also improve the calculated results.

Pseudolocal motions of guest molecules in organic and inorganic crystals have been identified as a dominant source of optical dephasing at low temperatures. Pseudolocal modes have also been discussed in connection with chromophores in small molecule organic glasses, such as ethanol.[42] Molecules in proteins such as heme in hemoglobin or chlorophyll in photosynthetic units undoubtedly undergo pseudolocal motions. It seems reasonable that any molecule in a solid in which the molecule is distinct from its surroundings will undergo pseudolocal motions. The nature of the motions will depend on the molecule and its environment, but in general the motions will be mixtures of translational and librational degrees of freedom. Since mechanical and electronic degrees of freedom are coupled, as evidenced by the pseudolocal mode optical dephasing, thermal excitations of local motions can play an important role in the properties and dynamics of molecules embedded in solid environments.

ACKNOWLEDGMENTS

The authors would like to thank the National Science Foundation Division of Materials Research (DMR 87-18959) for supporting this research. All calculations were performed on the IBM 3090 at the IBM Palo Alto Scientific Center.

[1] *Chemical and Biochemical Applications of Lasers*, edited by C. B. Moore (Academic, New York, 1976, 1977, 1978, 1979), Vols. 1–4.
[2] G. Fleming, *Chemical Application of Ultrafast Spectroscopy* (Oxford University, New York, 1986).
[3] *Applications of Picosecond Spectroscopy to Chemistry*, edited by K. R. Eisenthal (Reidel, Dordrecht, 1984).
[4] D. E. McCumber and M. D. Sturge, J. Appl. Phys. **34**, 1682 (1963).
[5] I. S. Osad'ko, Sov. Phys. Solid State **13**, 974 (1971); **14**, 2522 (1973); **17**, 2098 (1975); I. S. Osad'ko and S. A. Zhdanov, *ibid.* **18**, 441 (1976); I. S. Osad'ko, Sov. Phys. JETP **45**, 827 (1977); I. S. Osad'ko, S. A. Zhdanov, Sov. Phys. Solid State **19**, 982 (1977).
[6] C. B. Harris, J. Chem. Phys. **67**, 5607 (1977).
[7] G. J. Small, Chem. Phys. Lett. **57**, 501 (1978).
[8] P. de Bree and D. A. Wiersma, J. Chem. Phys. **70**, 790 (1979).
[9] J. L. Skinner and D. Hsu, Adv. Chem. Phys. **65**, 1 (1986).
[10] B. DiBartolo, *Optical Interactions in Solids* (Wiley, New York, 1968), Chap. 15.
[11] D. W. Pack and D. S. McClure, J. Chem. Phys. **87**, 5161 (1987).
[12] C. A. Walsh, M. Berg, L. R. Narasimhan, and M. D. Fayer, Acc. Chem. Res. **20**, 120 (1987).
[13] W. M. Hesselink and D. A. Wiersma, in *Spectroscopy and Excitation Dynamics of Condensed Molecular Systems*, edited by V. M. Agranovich and R. M. Hochstrasser (North Holland, Amsterdam, 1983).
[14] W. H. Hesselink and D. A. Wiersma, J. Chem. Phys. **73**, 648 (1980).
[15] F. G. Patterson, W. L. Wilson, H. W. H. Lee, and M. D. Fayer, Chem. Phys. Lett. **110**, 7 (1984).
[16] S. Ramdas, Chem. Phys. Lett. **60**, 320 (1979); K. Norris, P. Gray, D. P. Craig, C. P. Mallett, B. R. Markey, Chem. Phys. **79**, 9 (1983); D. P. Craig, B. R. Markey, A. O. Griewank, Chem. Phys. Lett. **62**, 223 (1979).
[17] T. R. Koehler, J. Chem. Phys. **72**, 3389 (1980); T. R. Koehler and J. Schmidt, Chem. Phys. Lett. **75**, 38 (1980).
[18] R. F. Loring, H. C. Anderson, and M. D. Fayer, J. Chem. Phys. **81**, 5395 (1984); R. J. Gulotty, C. A. Walsh, F. G. Patterson, W. L. Wilson, and M. D. Fayer, Chem. Phys. Lett. **125**, 507 (1986); L. Root and J. L. Skinner, J. Chem. Phys. **81**, 5310 (1984).
[19] R. W. Olson, H. W. H. Lee, F. G. Patterson, and M. D. Fayer, J. Chem. Phys. **76**, 31 (1982).
[20] B. J. McArdle, J. N. Sherwood, and A. C. Damask, J. Cryst. Growth **22**, 193 (1974).
[21] D. H. Spielberg, R. A. Arndt, A. C. Damask, and I. Lefkowitz, J. Chem. Phys. **54**, 2597 (1971).
[22] L. Colombo, A. E. Stanley, and J. R. Durig, J. Mol. Struct. **118**, 119 (1984); L. Colombo, Chem. Phys. Lett. **48**, 166 (1977).
[23] S. C. Ganguly and N. K. Choudhury, J. Chem. Phys. **21**, 554 (1953).
[24] H. deVries and D. A. Wiersma, J. Chem. Phys. **70**, 5807 (1979).
[25] A. Grimison, Theoret. Chim. Acta **20**, 263 (1971).
[26] R. Kulver and C. J. Eckhardt, Phys. Rev. B **37**, 5351 (1988).
[27] R. Ostertag and H. C. Wolf, Phys. Stat. Sol. **31**, 139 (1969).
[28] E. P. Burke and G. J. Small, J. Chem. Phys. **61**, 4588 (1974).
[29] H. W. H. Lee and M. D. Fayer, J. Chem. Phys. **84**, 5463 (1986).
[30] J. Godec and L. Colombo, J. Chem. Phys. **65**, 4693 (1975).
[31] B. Dorner, E. L. Bokhanov, S. L. Chaplot, J. Kalus, I. Natkanioc, G. S. Pawley, U. Schmelzer, and E. F. Sheka, J. Phys. C **15**, 2353 (1982).
[32] B. Gabrys, J. Higgins, and D. A. Young, Polymer **26**, 355 (1985); K. G. Conn, P. A. Beckmann, C. W. Mallory, and F. B. Mallory, J. Chem. Phys. **87**, 20 (1987).
[33] M. I. Kay, Y. Okaya, and D. E. Cox, Acta Cryst. B **27**, 26 (1971).
[34] R. Mason, Acta Cryst. **17**, 547 (1964), Table 4b (mean), 4c, and 4d.
[35] P. J. Cox and G. A. Sim, Acta Cryst. B **35**, 404 (1979).
[36] W. R. Busing, WMIN, *A Computer Program to Model Molecules and Crystals in Terms of Potential Energy Functions*, ONRL-5747 (1981), Oak Ridge National Laboratory, Oak Ridge, TN 37831.
[37] D. E. Williams, J. Chem. Phys. **45**, 3770 (1966).
[38] E. B. Wilson, Jr., J. C. Decius, and P. C. Cross, *Molecular Vibrations* (McGraw–Hill, New York, 1955).
[39] C. G. de Kruif, J. Chem. Thermodyn. **12**, 243 (1980).

[40]J. M. Ziman, *Principles in the Theory of Solids* (Cambridge University, Cambridge, 1972), p. 71.
[41]T. L. Starr and D. E. Williams, Acta Cryst. A **33**, 771 (1977); V. Schettino and S. Califano, J. Mol. Struct. **100**, 459 (1983).
[42]C. A. Walsh, M. Berg, L. R. Narasimhan, and M. D. Fayer, J. Chem. Phys. **86**, 77(1987); M. Berg, C. A. Walsh, L. R. Narasimhan, K. A. Littau, and M. D. Fayer, J. Chem. Phys. **88**, 1564 (1988); L. R. Narasimhan, D. W. Pack, and M. D. Fayer, Chem. Phys. Lett. **152**, 287 (1988).